



# Experimental and numerical study on thermoelectric liquid cooling module performance with different heat sink configurations

Paisarn Naphon<sup>1</sup> · Songkran Wiriyasart<sup>1</sup> · Chutichai Hommalee<sup>1</sup>

Received: 16 September 2018 / Accepted: 13 February 2019 / Published online: 21 February 2019  
© Springer-Verlag GmbH Germany, part of Springer Nature 2019

## Abstract

In the present study, the cooling performance of thermoelectric cooling module with different heat sink configurations has been investigated. In experiments, 0.015 kg/s cold water flow rate and hot water temperature are test in the range of 32–50 °C. Effects of heat sink configurations and hot side temperature on cooling performance of the thermoelectric cooling module are considered. For numerical study, a three-dimensional single-phase flow model is used to analyze the heat transfer and flow characteristics of the problem. The predicted results are verified with the measured data and good agreement is obtained. It can be found that the heat sink configurations have a significant effect on the velocity and temperature distributions of coolant which results in cooling performance of thermoelectric cooling module. The heat sink model C gives the highest cooling performance as compared with others models. While the higher hot water temperature results in increasing temperature different between hot and cold sides of thermoelectric plate. Therefore, cooling performance tends to decrease with increasing hot water temperature. The results from this study are expected to lead to guidelines that will allow designing the thermoelectric cooling module embedded with the heat sink to maximize cooling performance.

## Nomenclature

$C_1, C_2$	Closure coefficients for the turbulence equation
$C_p$	Specific heat of coolant, [kJ kg <sup>-1</sup> K <sup>-1</sup> ]
$k$	Thermal conductivity, [Wm <sup>-1</sup> K <sup>-1</sup> ]
$k$	Turbulence kinetic energy
$m$	Mass flow rate, [kg s <sup>-1</sup> ]
$P$	Pressure, [kPa]
$Q$	Heat dissipation, [W]
$q''$	Heat flux, [Wm <sup>-2</sup> ]
$R$	Thermal resistance, [°CW <sup>-1</sup> ]
$T$	Temperature, [K]
$u, v, w$	Velocity components in transformed plane, [ms <sup>-1</sup> ]
$V_{in}$	Inlet velocity, [ms <sup>-1</sup> ]

## Greek symbols

$\varepsilon$	Turbulent energy dissipation rate, [m <sup>2</sup> s <sup>-3</sup> ]
$\rho$	Density, [kgm <sup>-3</sup> ]
$\mu_l, \mu_t$	Laminar and turbulent viscosity, [N.sm <sup>-2</sup> ]
$\nu$	Kinematic viscosity, [m <sup>2</sup> s <sup>-1</sup> ]
$\sigma_k, \sigma_\varepsilon$	Empirical constants in turbulence model equations

## Subscripts and superscripts

<i>base</i>	Base
<i>in</i>	Inlet
<i>out</i>	Outlet
<i>wall</i>	Wall
<i>s</i>	Solid

## 1 Introduction

Today, a thermoelectric cooler has been continuously developed to achieve many applications. Cold and hot sides of the thermoelectric are developed and utilized, especially, the most practice typically used to enhance cooling capacity in electronic components. On the other hand, the cold and hot sides of thermoelectric are a function of power input. Generally, the works reported on the thermoelectric applications in various systems. Gurevich and Lashkevych [1] investigated the physical peculiarities of the thermoelectric cooling phenomenon by an electric current in p–n structures of thermally thick structure in the linear approximation. Naphon et al. [2, 3] experimentally and numerically investigated the fluid flow and heat transfer in the mini-rectangular fin and micro-channel heat sinks for cooling CPU of PC. Some study presented the thermal performance of a thermoelectric water-cooling device for electronic equipment as the heat load below 57 W

✉ Paisarn Naphon  
paisarnn@g.swu.ac.th

<sup>1</sup> Thermo-Fluids and Heat Transfer Enhancement Laboratory (TFHT), Department of Mechanical Engineering, Faculty of Engineering, Srinakharinwirot University, 63 Rangsit-Nakhornnayok Rd., Ongkharak, Nakhorn-Nayok 26120, Thailand

(Huang et al. [4]). Gould et al. [5] demonstrated the thermoelectric cooling and micro-power generation from waste heat within a standard desktop computer. Most of the previous studies on this area have been considered a generalized theoretical model for the optimization of a thermoelectric cooling system (Zhou and Yu. [6]; He et al. [7]; Wang et al. [8]; Chen et al. [9]; Liu et al. [10]). They analyzed the maximum coefficient of performance (COP) and the maximum cooling capacity of the TEC system which the finite total thermal conductance is optimally allocated. In addition, a prototype thermoelectric system integrated with phase change material heat storage unit for space cooling has been developed (Zhao and Tan. [11]). The experimental test in a reduced-scale chamber has achieved 7 °C temperature difference between “indoor” and “outdoor” environments and realized an average cooling COP of 0.87 for the thermoelectric cooling system, with the maximum cooling COP of 1.22. There were some papers presented on the development the thermoelectric generator model coupled with exhaust and cooling channels for an exhaust-based TEG (ETEG) system (Du et al. [12]). The influence of the cooling type, coolant flow rate, length, number and location of bafflers, and flow arrangement had been investigated. It was found that the net output power was generally higher with liquid cooling than air cooling. Some of study reporting of thermoelectric model system on the various cooling systems had been continuously performed (Hu et al. [13]; Kiflemarian et al. [14]; Kwon et al. [15]; Liu et al. [16]; Tan and Zhao. [17]; Ahammed et al. [18]; Cai et al. [19]). They proposed the two-stage thermoelectric cooling module (TEM) and explored in detail an arrangement with primary and secondary heat paths to guide heat flow to the thermoelectric generator (TEG) modules and heat sink. Experimental results showed that for the highest heat input, the temperature of the device can be reduced by 20–40% as compared to natural convection case. Some work considered an advanced mathematical model that uses multi-element thermoelectric components connected in series and considered internal and external irreversibility and also the temperature gradients along the flow direction (He et al. [20]; Kiflemarian et al. [21]), however, there was paper reported the combining analytical system model and artificial neural networks (ANN) as well as the dynamic calculation functions of internal parameters of TEM which it was found that the optimum thickness of aluminum panel and insulation were around 1–2 mm and 40–50 mm, respectively (Luo et al. [22]). Ma and Yu [23] experimentally investigated the cooling characteristics of a realistic thermoelectric module that operates under single and continuous square current pulse. Cooling temperature in each current pulse showed an increasing trend similar to that of a first order

step response. The cooling characteristics under different cooling loads were quite similar, except for the different initial temperatures. Qian and Ren [24] considered the cooling performance of thermoelectric module. The hypothetical transverse thermoelectric devices were constructed from alternating layers of a bismuth telluride based thermoelectric material and pure metals. Cai et al. [25] applied the thermoelectric heat exchanger for CPU cooling. The optimization based on thermoelectric heat exchanger module (TEHEM) is presented for application in CPU cooler. The supplied pulse currents to the hot and the cold stage of a two-stage cascaded TEC to seek in temperature drop across the TEC had been considered by Gao et al. [26]. Ibañez-Puy et al. [27] studied a vertical configuration of 16 TE modules as a heating and cooling system for residential buildings. Based on the measured data, it had been demonstrated that the system can be successfully installed as a heating or cooling system in buildings. Tests have confirmed the huge relevance of the temperature difference between the two sides of the cells, taking especial relevance in the cooling mode. Joshi et al. [28] applied the thermoelectric cooling module in the portable flesh water generator based on the fundamental of thermoelectric cooling effect by condensing the moisture from the ambient moist air. Some of papers presented on the integrated heat pipe with thermoelectric for electronic cooling (Liu et al. [29]; Sun et al. [30]). A thermoelectric cooling (TEC) system had been proposed to remove the heat that was generated by electronic device. To improve the performance of this system, a gravity assistant heat pipe (GAHP) was attached on the hot side of the thermoelectric cooling module, serving as a heat sink. Su et al. [31] proposed a free-standing planar design of thermoelectric microrefrigerator based on thin film technologies to address the high-performance on chip cooling and compatibility with microelectronics fabrication.

According reviewed papers, the most researchers investigated on the application of thermoelectric in various applications which the relevant parameters have significant effect on the thermal performance of thermoelectric. Therefore, the relevant parameters should be optimized to obtain the maximum cooling performance of the thermoelectric. The objective of this study is to optimize the relevant parameters; the heat sink configurations embedded to the thermoelectric cooling module and hot side temperature of the thermoelectric for obtaining maximum cooling capacity of thermoelectric cooling module. In addition, the numerical results are verified with the measured data. The results from this study are expected to lead to guidelines that will allow designing the thermoelectric cooling module for cooling electric devices with maximum cooling capacity.

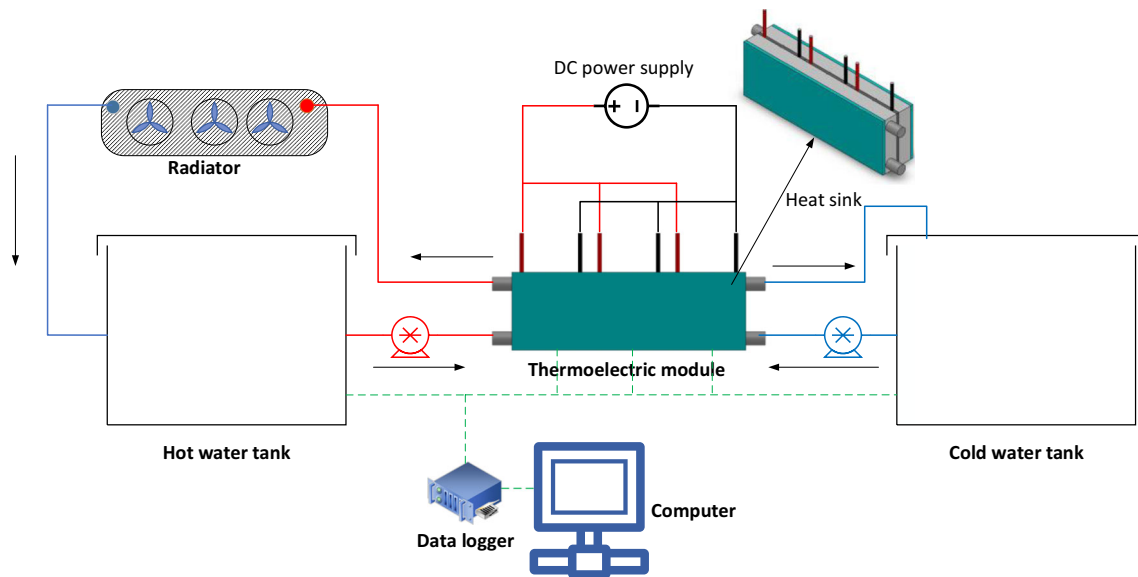


Fig. 1 Schematic illustration of the thermoelectric cooler system

## 2 Experimental apparatus and test procedure

### 2.1 Experimental apparatus

The experimental apparatus of the thermoelectric cooling module is shown in Fig. 1. The test loop is divided into two loops; hot water loop and cold water loop. The cold water loop is consisted of water pump, cold water tank, cold water block while hot water loop is consisted of hot water block, water pump, hot water tank and radiator. The thermoelectric cooling module is consisted of three parts; hot water block, cold water block, and thermoelectric plate. The hot and cold water blocks are fabricated from aluminium with a longitudinal fins heat sink. Inlet hot and cold water temperatures are measured with Type-T thermocouples with an accuracy of 0.1% of full scale. Hot and cold surface temperatures of thermoelectric plates are measured with six thermocouples as shown in Fig. 2. All types T thermocouples are pre-calibrated with dry block

temperature calibrator with 0.01 °C precision. The mass flow rate of hot and cold water are measured by flow meter sensor of an accuracy of 0.01% of full scale.

### 2.2 Test section

The thermoelectric cooling module is consisted of hot and cold water blocks and three thermoelectric plates with dimension of  $40 \times 40$  mm as shown in Fig. 2. Dimension of three different water block models are shown in Fig. 3. The voltage and current of 12 V, 10A are supplied for each thermoelectric plates. Hot and cold water blocks are attached with other sides of three thermoelectric plates with high thermal conductivity special glue. The hot and cold water flowing inside water blocks are in countercurrent direction arrangements. The water block is fabricated from aluminium with a longitudinal fins with dimension of  $10 \times 40 \times 120$  mm. Two water pumps are used to circulate hot and cold water that flow separately

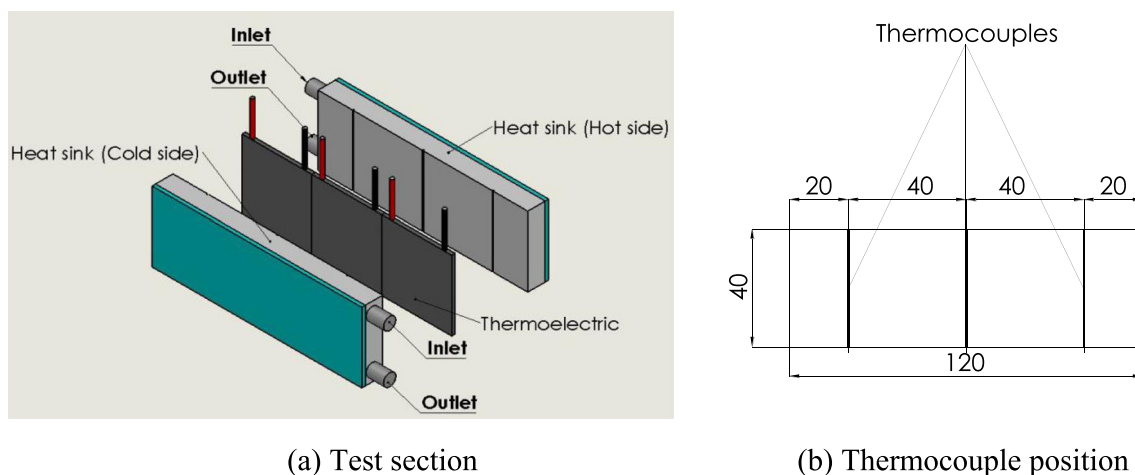
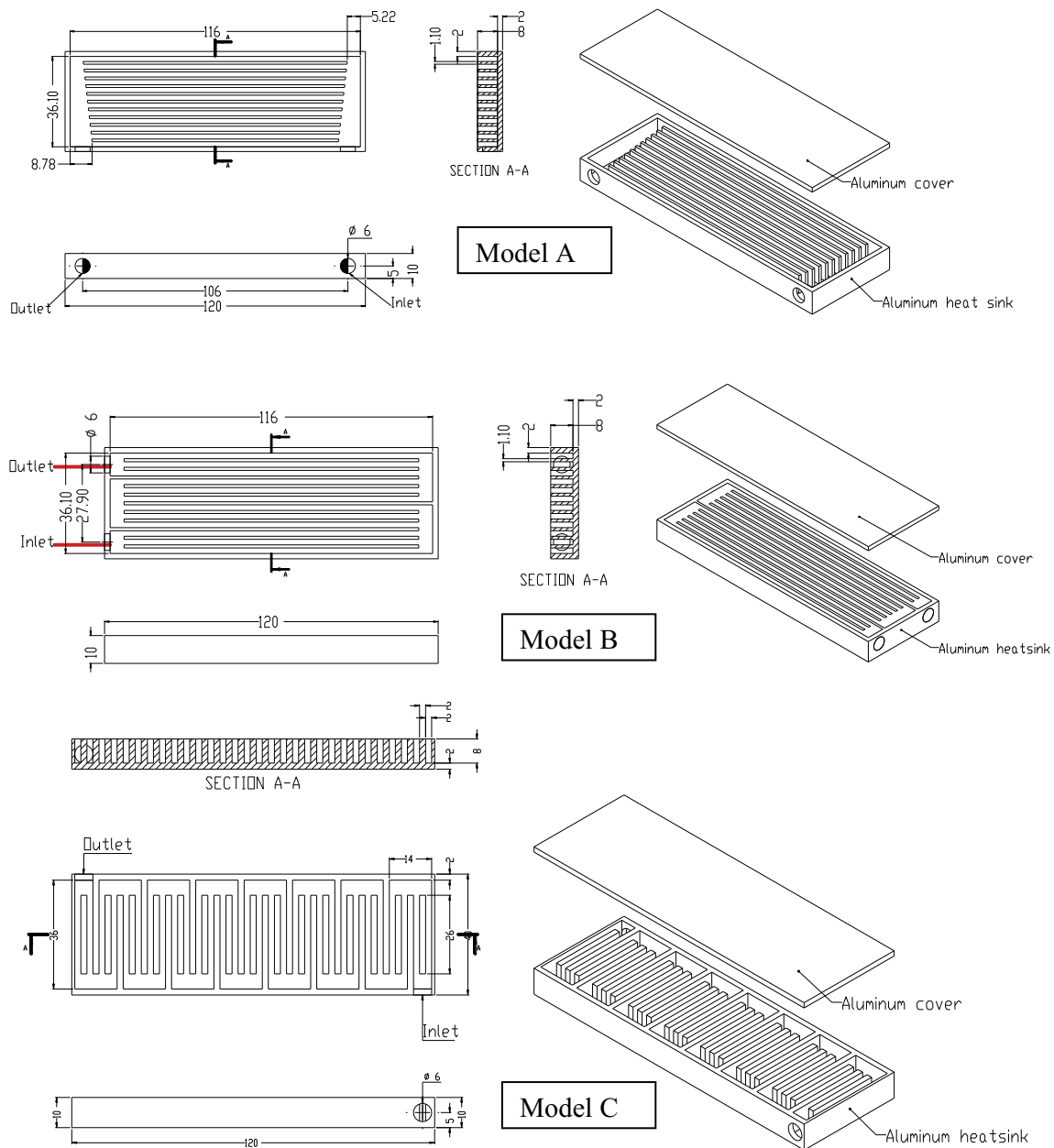


Fig. 2 Schematic diagram of a thermoelectric cooler module b thermocouples positions



**Fig. 3** Schematic of the various heat sinks used in the present study

through the water blocks. The heat sink surface is machined with straight grooves of  $1 \text{ mm} \times 1 \text{ mm}$  (width  $\times$  depth) which installed three thermocouples to measure temperature. The temperature at various positions such as water inlet, water outlet and heat source temperature are recorded in five times using data acquisition system.

### 2.3 Experimental test method and uncertainty analysis

In experiments, the hot and water mass flow rate are kept constant at  $0.015 \text{ kg/s}$ . For a specific hot water temperature in radiator at  $32, 40, 50 \text{ }^\circ\text{C}$ , the cold water

temperature has been recorded in five times with data acquisition system for 45 min. All instruments are also pre-calibrated. Uncertainty estimates can be done by considering the errors of the instruments, the measurement variance and calibrations errors. The uncertainty in the measured temperature is estimated to be less than  $\pm 0.1 \text{ }^\circ\text{C}$ . The accuracy and uncertainties of the instruments are shown in the Table 1. The thermal resistance of the heat sink can be calculated from:

$$R = \frac{T_{\text{base}} - T_{\text{in}}}{mC_p(T_{\text{in}} - T_{\text{out}})} \quad (1)$$

**Table 1** Accuracy and uncertainty of measurements

Instrument	Accuracy (%)	Uncertainty
Power supply, V	0.2	±0.5
Thermocouple type T	0.1	±0.1
Data logger (°C)	0.1	±0.1
Multi-meter	0.1	±0.05

$$\text{Uncertainty of } R_{\text{heatsink}} = \sqrt{\left(\frac{\partial R_{\text{heatsink}}}{\partial T_{\text{base}}} \Delta T_{\text{base}}\right)^2 + \left(\frac{\partial R_{\text{heatsink}}}{\partial T_{\text{in}}} \Delta T_{\text{in}}\right)^2 + \left(\frac{\partial R_{\text{heatsink}}}{\partial m} \Delta m\right)^2 + \left(\frac{\partial R_{\text{heatsink}}}{\partial T_{\text{out}}} \Delta T_{\text{out}}\right)^2} \quad (2)$$

### 3 Mathematical model

#### 3.1 Geometrical model

Based on experimental works, a validation process of the numerical model is performed. The geometrical model for this study is the cold water block with details as shown in Fig. 3. Although low Reynolds number but due to high turbulent intensity flowing through the heat sink with various flow channel configurations, a single-phase flow model with three-dimensional has been applied to analyze the heat transfer and flow characteristics of the problem. In general, there are many turbulent models such as large eddy simulation, Reynolds Stress Model and direct numerical simulation can be simulated the problem, however, these models require more time consuming and lot of computer resources. In the present study, therefore, the standard  $k$ - $\varepsilon$  turbulent model is employed to simulate the problem. The cold water block is fabricated from aluminium with dimensions of  $120 \times 40 \times 10$  mm, a fin thickness of 8 mm, and a cover thickness of 4.5 mm. The cold water block is attached with the thermoelectric plates to absorb the heat and then continuous cooled by liquid coolant with mass flow rate of 0.015 kg/s. The diameter of inlet and outlet ports are 5 mm. The governing equations of the mass, momentum and energy are applied with the following assumptions;

- Adiabatic surface for all of free wall surfaces except bottom wall surface for constant wall temperature.
- Single phase and incompressible flow
- Negligible gravitational force and constant properties of coolant
- Negligible radiation heat transfer
- Negligible contract resistance at the interfaces between the solid wall and the coolant

Where  $T_{\text{base}}$ , is the base temperature of the heat sink and  $T_{\text{in}}$  is inlet coolant temperature passing through the heat sink. Based on the Coleman and Steele [32], the uncertainties of the relevant parameters obtained from the data reduction process are calculated with the maximum uncertainties of the thermal resistance is  $\pm 5.0\%$ . The maximum uncertainty of the thermal resistance can be determined from

#### 3.2 Main governing eqs

A single phase model is based on the numerical solution of the governing equations of the mass, momentum and energy equations as follows [33, 35];

Continuity equation:

$$\frac{\partial \rho \bar{u}_i}{\partial x_i} = 0 \quad (3)$$

Momentum equation:

$$\rho \bar{u}_j \frac{\partial \bar{u}_i}{\partial x_j} = -\frac{\partial \bar{p}}{\partial x_i} + \frac{\partial}{\partial x_j} \left( \mu_t \left( \frac{\partial \bar{u}_i}{\partial x_j} + \frac{\partial \bar{u}_j}{\partial x_i} \right) - \rho \bar{u}_i \bar{u}_j \right) \quad (4)$$

Energy equation for fluid:

$$\rho \bar{u}_j \frac{\partial \bar{T}}{\partial x_j} = \frac{\partial}{\partial x_j} \left( \left( \frac{\mu_l}{\sigma_l} + \frac{\mu_t}{\sigma_t} \right) \frac{\partial \bar{T}}{\partial x_j} \right) \quad (5)$$

Energy equation for solid:

$$\frac{\partial}{\partial x_i} \left( k_s \frac{\partial T}{\partial x_i} \right) = 0 \quad (6)$$

Transport equations for turbulence kinetic energy ( $k$ ):

$$\rho \bar{u}_j \frac{\partial k}{\partial x_j} = \frac{\partial}{\partial x_j} \left[ \left( \mu_l + \frac{\mu_t}{\sigma_k} \right) \frac{\partial k}{\partial x_j} \right] + \mu_t \left( \frac{\partial \bar{u}_i}{\partial x_j} + \frac{\partial \bar{u}_j}{\partial x_i} \right) \frac{\partial \bar{u}_i}{\partial x_j} - \rho \varepsilon \quad (7)$$

Transport equations for turbulence kinetic energy dissipation ( $\varepsilon$ ):

$$\rho \bar{u}_j \frac{\partial \varepsilon}{\partial x_j} = \frac{\partial}{\partial x_j} \left[ \left( \mu_l + \frac{\mu_t}{\sigma_\varepsilon} \right) \frac{\partial \varepsilon}{\partial x_j} \right] + C_1 \mu_t \frac{\varepsilon}{k} \left( \frac{\partial \bar{u}_i}{\partial x_j} + \frac{\partial \bar{u}_j}{\partial x_i} \right) \frac{\partial \bar{u}_i}{\partial x_j} - C_2 \rho \frac{\varepsilon^2}{k} \quad (8)$$

Where:

$$\mu_t = \rho C_\mu \frac{k^2}{\varepsilon} \tag{9}$$

The empirical constants for the turbulence model are arrived by comprehensive data fitting for a wide range of turbulent flow of Launder and Spalding [33, 34]:

$$C_1 = 1.44, C_2 = 1.92, C_\mu = 0.09, \sigma_k = 1.0, \sigma_\varepsilon = 1.3$$

### 3.3 Boundary conditions

Bottom wall of the cold water block:

$$T = T_{wall} \tag{10}$$

Surrounding walls surfaces:

$$\frac{\partial T}{\partial x} = 0 \tag{11}$$

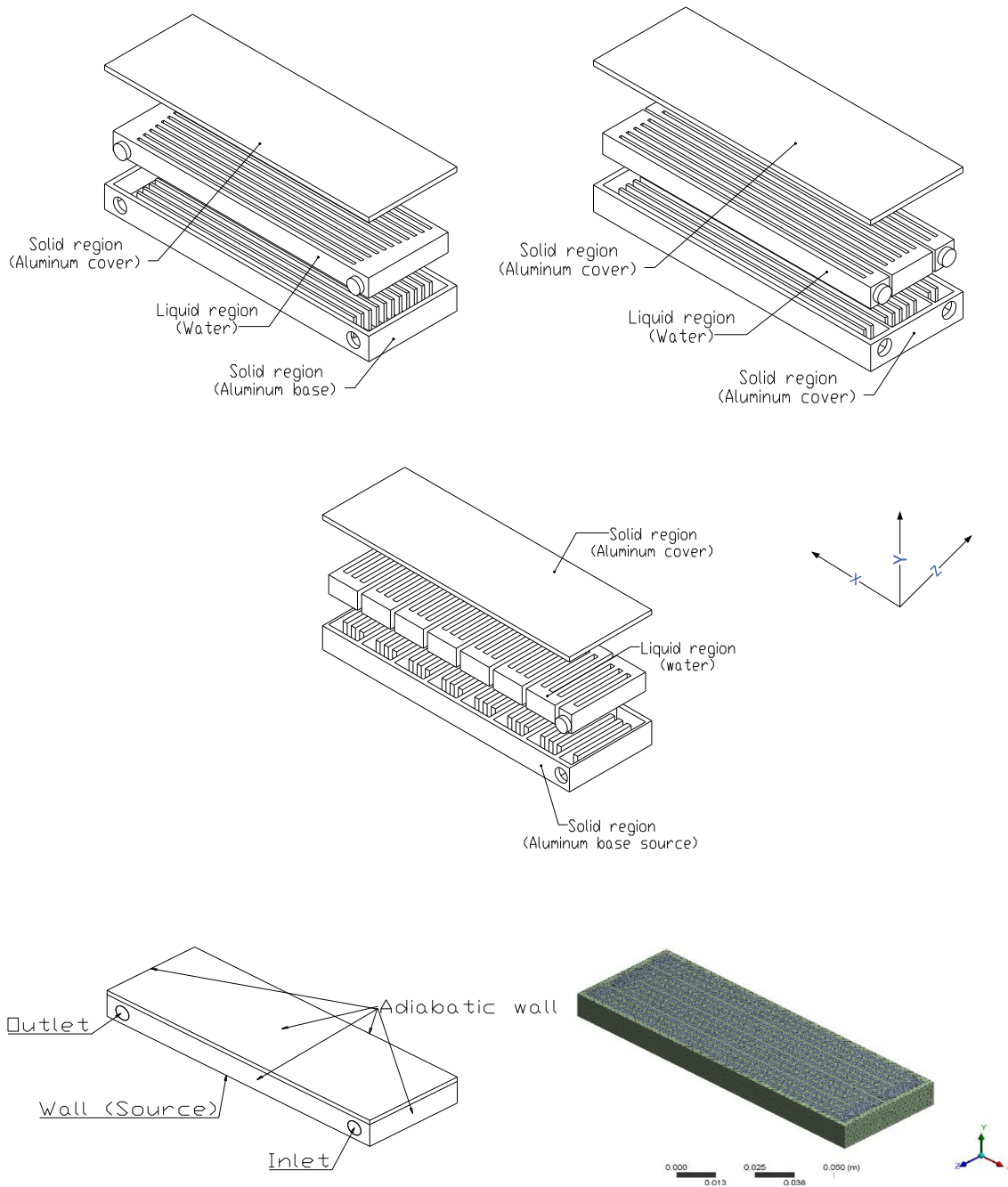


Fig. 4 Computational domain of various heat sinks used in the present study

Inlet port:

$$T = T_{in}, V = V_{in} \tag{12}$$

Outlet port:

$$p = p_{out} \tag{13}$$

Coolant-solid interface:

$$-k_l \frac{\partial T_l}{\partial x} = -k_s \frac{\partial T_s}{\partial x} \tag{14}$$

### 3.4 Grid independent tests

In the numerical study, the computational domain used in the present study is shown in Fig. 4. The cold water block is divided into 3 sections; cold plate base with longitudinal fins, Fluid (coolant), and upper cover plate. Based on the control volume method, SIMPLEC algorithm of Van Doormal and Raithby [36] is employed to deal with the problem of velocity and pressure coupling. Inlet coolant temperature with uniform velocity entering the test section is applied. The mesh geometries are generated as shown in Fig. 4. Based on the water block model C, in order to assess the accuracy of these computations based on the computational grids of  $2.6 \times 10^5$ ,  $3.00 \times 10^5$ , and  $3.4 \times 10^5$  are used to test the grid independence of the solution (Outlet water temperature). As shown in Table 2, the outlet water temperature of  $3.4 \times 10^5$  is finer than that from  $3.00 \times 10^5$  within 1%. Therefore, the grid number of  $3.00 \times 10^5$  ensures a satisfactory solution. The relevant results are obtained when the normalized residual falls below  $10^{-5}$  for all variables. The commercial program ANSYS/FLUENT has been employed as the numerical solver. The computer used for calculation in this study is a dual CPUs socket 1366 of 12cores-24threads, the memory are totally 64 GB of frequency 1333 MHz.

**Table 2** Grid independent test

Models	Number of grids	$T_{w,out}$	%Errors
A	256,000	24.58	–
	289,000	25.10	2.09
	334,000	25.27	0.68
B	257,000	22.46	–
	299,000	23.23	3.37
	339,000	23.49	0.94
C	260,00	22.93	–
	300,000	23.60	2.88
	340,000	23.61	0.63

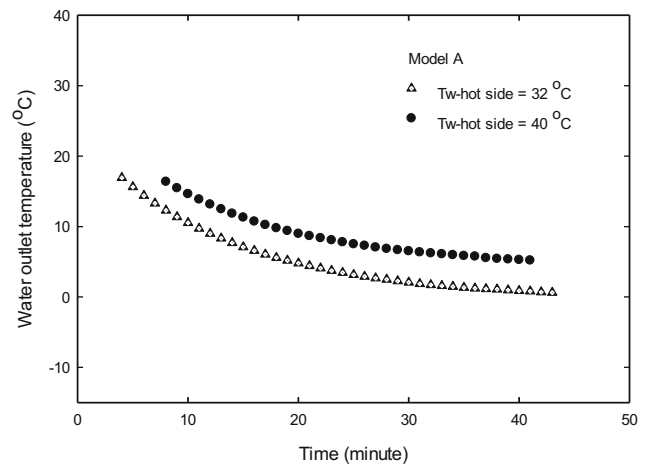


**Fig. 5** Variation of cold water outlet temperature of model A vs time at hot side of 32 and 40 °C

### 4 Results and discussion

Figure 5 shows the variation of cold water temperature with time obtained from thermoelectric cooling module with different hot side water temperatures of 32 °C and 40 °C. Experiments are performed on the constant input power of 60 W. For a specific hot side water temperature at radiator, it can be seen that the cold water temperature tends to decrease with increasing time.  $T_{w-hot} = 32 \text{ °C}$  gives the cold water temperature lower than those from  $T_{w-hot} = 40 \text{ °C}$ . This means that the cooling performance of the thermoelectric cooling module increases with decreasing hot water temperature. Due to higher hot water temperature, the heat dissipation from the hot side thermoelectric cooling module decreases which results in the drop of cold water temperature as shown in Fig. 5.

Figure 6 shows the variation of cold water temperature with time for different cold water blocks models. From Fig. 4, the water flows through one fin pass and four fin pass for model A, model B, respectively. It can be seen that the cold water temperature obtained from water block model B are lower

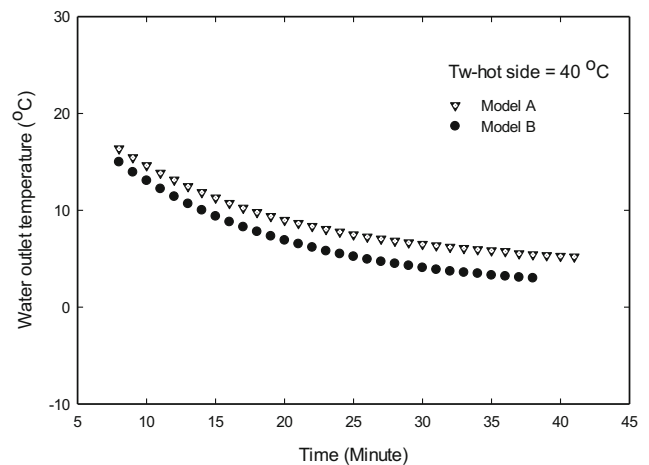


**Fig. 6** Variation of cold water outlet temperature of model A and B vs time at hot side of 40 °C

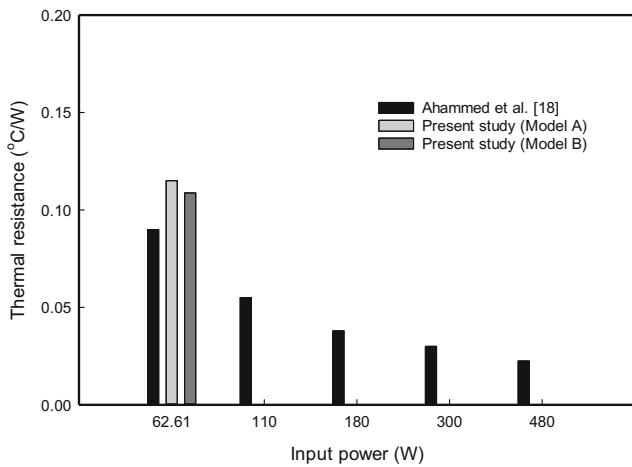


Fig. 7 Comparison of thermal resistance from the present study and Ahammed et al. [18]

than those from water block model A which results in lower thermal resistance. This means that the water block model B gives the cooling performance higher than that model A. The results obtained from the present study are compared with those from other researchers [18] as shown in Fig. 7. It can be seen that the thermal resistance obtained from the present study are higher than those from Ahammed et al. [18]. This is because the heat sinks with different configurations and test conditions are performed. In addition, the thermal resistance tends to decrease with increasing input power [18].

Due to there is not the paper presented on the heat and flow through the water block with the same conditions. Therefore, the predicted flow and heat transfer behaviors in the water block with different configurations obtained from are compared with the present experiment. Figure 8 shows the comparison between the measured outlet cold water temperature and the predicted results for the water block model B. It can be seen that clearly seen from figure that the results obtained from the model slightly underpredict the measured data and

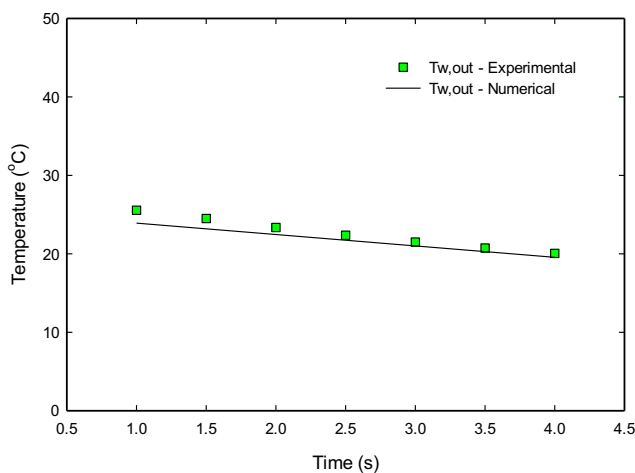


Fig. 8 Comparison between the measured data and predicted results

the average difference between the measured data of 2.5%. The results of the velocity and temperature distributions obtained from water blocks with different heat sink configurations are shown in Figs. 9 and 10, respectively. The cold water and hot water flow entering cold and hot water blocks which attached on the cold and hot surfaces of three thermoelectric plates. For a specific hot side water temperature, the cooling performance of the thermoelectric cooling module is determined by using cold water loop system entering the cold water block. In general, based on the operating conditions of

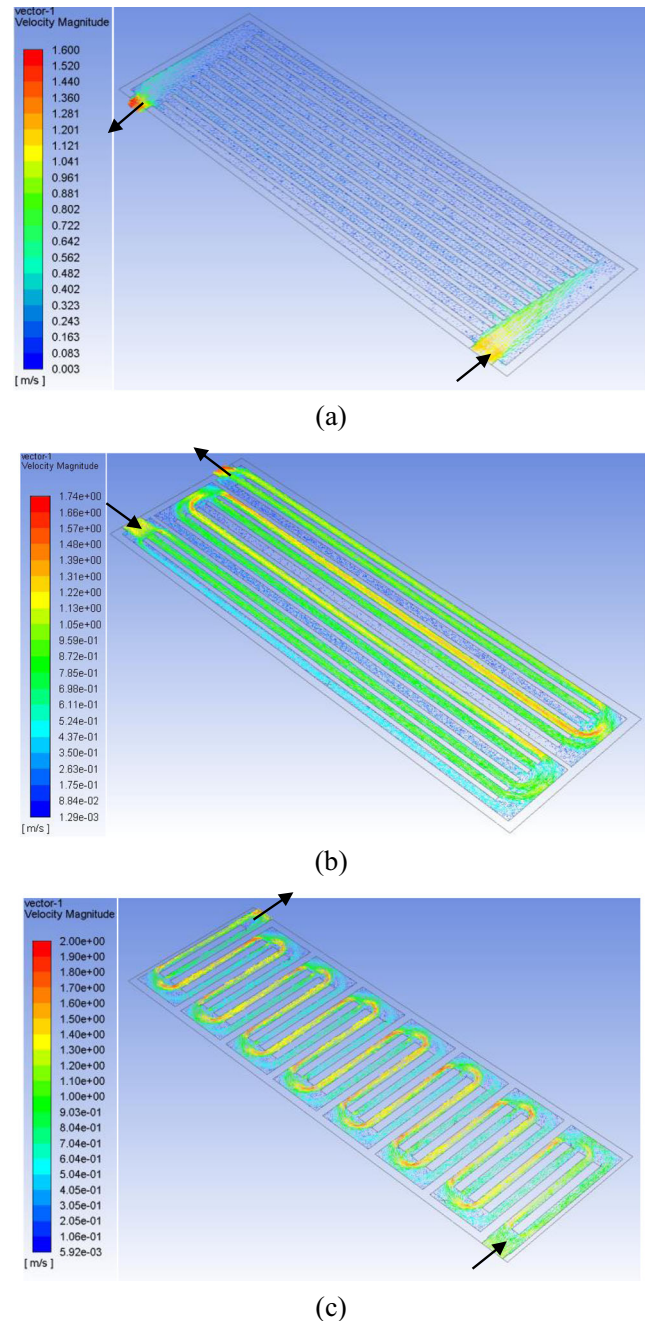
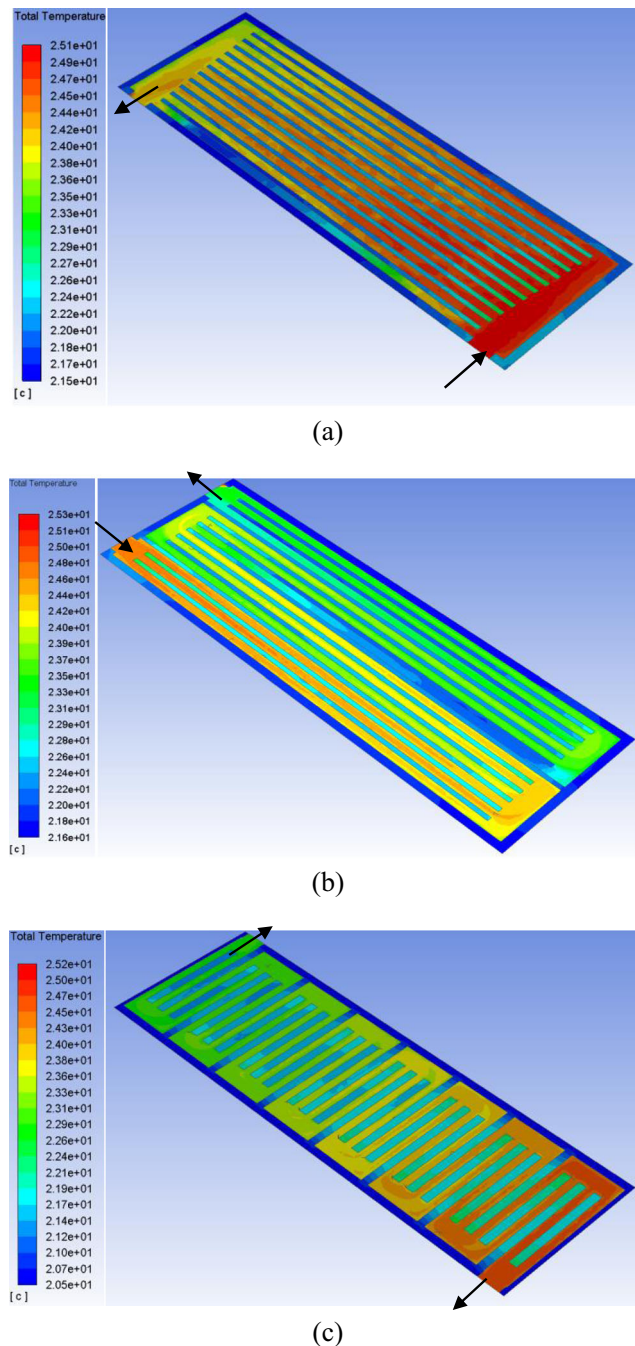


Fig. 9 Variation of velocity vector of heat sink a model A b model B c model C



thermoelectric cooler module with constant input power, average temperature of hot and cold plate sides of thermoelectric are recorded in the period time of 40 min. It is difficult to obtain the generated heat at the thermoelectric surface, therefore, the numerical study is performed under average constant temperature at any time on the rear face of the water block. In order to obtain the numerical results, the calculations are performed for fluid flow in the cold water block with the longitudinal fins heat sink with different configurations. To



**Fig. 10** Variation of temperature contour of heat sink **a** model A **b** model B **c** model C

consider the fluid flow structure and temperature distributions flowing through the longitudinal fins heat sink, these results are shown in Figs. 9 and 10, respectively. The overall fluid flow field at the inlet plenum, longitudinal fin heat sink and outlet plenum of different water block configurations are shown in Fig. 9. From the water block model A, the coolant flow into the water blocks as once through pass. A flow pattern at the inlet plenum has a significant effect on the velocity distribution and direction of fluid flow in the longitudinal fins heat sink. After the fluid flows into the inlet port of the water block, the fluid spreads out and flows into the longitudinal fins heat sink in X-direction. The main fluid flows in the inner region and some fluid flowing in the outer region as shown in Fig. 9a. Based on the velocity distribution, it can be seen that the flow velocity is not uniformity which non-uniformity of the fluid flow which results in the temperature distribution of the coolant flowing through the heat sink as shown in Fig. 10. For the water block model B, the coolant flows entering the water block with heat sink inside as four passes before flows out the water block. In each pass channel, there are two longitudinal fins are attached along the length as shown in Fig. 3. For the water block model C, the coolant flows entering the water block with heat sink inside as fifteen passes before flows out the water block. In each pass channel, there are a longitudinal fin are attached along the width as shown in Fig. 3. It can be seen that the flow distributions obtained from three water block models are not uniformity and temperature distributions which results significant effect on the cooling performance. In addition, it can be seen that the cooling performance the water block model C is higher than that of the water block model B and model A, respectively.

## 5 Conclusions

In the present study, an evaluation of the cooling performance of thermoelectric cooling module embedded with different heat sink configurations are investigated experimentally and numerically. A three-dimensional single-phase flow model is used to analyze the heat transfer and flow characteristics of the problem under transient conditions. From the results, it is found that the predicted results are reasonable agreement with the experimental data. The cooling performance of the thermoelectric cooling module depends hot side water temperature. While the heat sink configurations have a significant effect on the flow and temperature distributions of coolant flowing inside the water block and then cooling performance. The water block model C gives the highest cooling performance as compared with other models. The obtained results are expected to guideline that will allow designing the heat sink configuration for thermoelectric cooling module to maximize cooling capacity for cooling electronic devices.

**Acknowledgements** The authors would like to express their appreciation to the Excellent Center for Sustainable Engineering (ECSE) of the Srinakharinwirot University (SWU) for providing financial support for this study.

**Publisher's note** Springer Nature remains neutral with regard to jurisdictional claims in published maps and institutional affiliations.

## References

- Gurevich YG, Lashkevych I (2009) Non-typical temperature distribution in p–n structure under thermoelectric cooling. *Int J Therm Sci* 48(11):2080–2084
- Naphon P, Klangchart S, Wongwises S (2009) Numerical investigation on the heat transfer and flow in the mini-fin heat sink for CPU. *International Communications in Heat and Mass Transfer* 36(8):834–840
- Naphon P, Wiriyasart S (2009) Liquid cooling in the mini-rectangular fin heat sink with and without thermoelectric for CPU. *International Communications in Heat and Mass Transfer* 36(2):166–171
- Huang HS, Weng YC, Chang YW, Chen SL, Ke MT (2010) Thermoelectric water-cooling device applied to electronic equipment. *International Communications in Heat and Mass Transfer* 37(2):140–146
- Gould CA, Shammas NYA, Grainger S, Taylor I (2011) Thermoelectric cooling of microelectronic circuits and waste heat electrical power generation in a desktop personal computer. *Mater Sci Eng B* 176(4):316–325
- Zhou Y, Yu J (2012) Design optimization of thermoelectric cooling systems for applications in electronic devices. *Int J Refrig* 35(4):1139–1144
- He W, Zhou J, Hou J, Chen C, Ji J (2013) Theoretical and experimental investigation on a thermoelectric cooling and heating system driven by solar. *Appl Energy* 107:89–97
- Wang X, Yu J, Ma M (2013) Optimization of heat sink configuration for thermoelectric cooling system based on entropy generation analysis. *Int J Heat Mass Transf* 63:361–365
- Chen WH, Wang CC, Hung CI (2014) Geometric effect on cooling power and performance of an integrated thermoelectric generation-cooling system. *Energy Convers Manag* 87:566–575
- Liu Z, Zhang L, Gong G (2014) Experimental evaluation of a solar thermoelectric cooled ceiling combined with displacement ventilation system. *Energy Convers Manag* 87:559–565
- Zhao D, Tan G (2014) Experimental evaluation of a prototype thermoelectric system integrated with PCM (phase change material) for space cooling. *Energy* 68:658–666
- Du Q, Diao H, Niu Z, Zhang G, Shu G, Jiao K (2015) Effect of cooling design on the characteristics and performance of thermoelectric generator used for internal combustion engine. *Energy Convers Manag* 101:9–18
- Hu HM, Ge TS, Dai YJ, Wang RZ (2015) Experimental investigation on two-stage thermoelectric cooling system adopted in isoelectric focusing. *Int J Refrig* 53:1–12
- Kiflemariam R, Lin C-X (2015) Numerical simulation of integrated liquid cooling and thermoelectric generation for self-cooling of electronic devices. *Int J Therm Sci* 94:193–203
- Kwon B, Baek SH, Kim SK, Hyun DB, Kim JS (2015) A differential method for measuring cooling performance of a thermoelectric module. *Appl Therm Eng* 87:209–213
- Liu D, Zhao FY, Yang HX, Tang GF (2015) Thermoelectric mini cooler coupled with micro thermosiphon for CPU cooling system. *Energy* 83:29–36
- Tan G, Zhao D (2015) Study of a thermoelectric space cooling system integrated with phase change material. *Appl Therm Eng* 86:187–198
- Ahamed N, Asirvatham LG, Wongwises S (2016) Thermoelectric cooling of electronic devices with nanofluid in a multiport minichannel heat exchanger. *Exp Thermal Fluid Sci* 74:81–90
- Cai Y, Liu D, Zhao FY, Tang J-F (2016) Performance analysis and assessment of thermoelectric micro cooler for electronic devices. *Energy Convers Manag* 124:203–211
- He W, Wang S, Lu C, Zhang X, Li Y (2016) Influence of different cooling methods on thermoelectric performance of an engine exhaust gas waste heat recovery system. *Appl Energy* 162:1251–1258
- Kiflemariam R, Lin CX (2016) Experimental investigation on heat driven self-cooling application based on thermoelectric system. *Int J Therm Sci* 109:309–322
- Luo Y, Zhang L, Liu Z, Wang Y, Wu J, Wang X (2016) Dynamic heat transfer modeling and parametric study of thermoelectric radiant cooling and heating panel system. *Energy Convers Manag* 124:504–516
- Ma M, Yu J (2016) Experimental study on transient cooling characteristics of a realistic thermoelectric module under a current pulse operation. *Energy Convers Manag* 126:210–216
- Qian B, Ren F (2016) Cooling performance of transverse thermoelectric devices. *Int J Heat Mass Transf* 95:787–794
- Cai Y, Liu D, Yang JJ, Wang Y, Zhao FY (2017) Optimization of thermoelectric cooling system for application in CPU cooler. *Energy Procedia* 105:1644–1650
- Gao YW, Lv H, Wang XD, Yan WM (2017) Enhanced Peltier cooling of two-stage thermoelectric cooler via pulse currents. *Int J Heat Mass Transf* 114:656–663
- Ibañez-Puy M, Bermejo-Busto J, Martín-Gómez C, Vidaurre-Arbizu M, Sacristán-Fernández JA (2017) Thermoelectric cooling heating unit performance under real conditions. *Appl Energy* 200:303–314
- Joshi VP, Joshi VS, Kothari HA, Mahajan MD, Chaudhari MB, Sant KD (2017) Experimental investigations on a portable fresh water generator using a thermoelectric cooler. *Energy Procedia* 109:161–166
- Liu D, Cai Y, Zhao FY (2017) Optimal design of thermoelectric cooling system integrated heat pipes for electric devices. *Energy* 128:403–413
- Sun X, Yang Y, Zhang H, Si H, Huang L, Liao S, Gu X (2017) Experimental research of a thermoelectric cooling system integrated with gravity assistant heat pipe for cooling electronic devices. *Energy Procedia* 105:4909–4914
- Su Y, Lu J, Huang B (2018) Free-standing planar thin-film thermoelectric microrefrigerators and the effects of thermal and electrical contact resistances. *Int J Heat Mass Transf* 117:436–446
- Coleman HW, Steele WG (1989) *Experimental and Uncertainty Analysis for Engineers*. John Wiley & Sons, New York
- Versteeg HK, Malalasekera W (1995) *Computational fluid dynamics*. Longman Group, New York
- Oosthuizen PH, Nayler D (1999) *An introduction to convective heat transfer analysis*. Mc-Graw-Hill, New York
- Lauder BE, Spalding DB (1973) *Mathematical models of turbulence*. Cambridge Academic Press, Cambridge
- Van Doormal JP, Raithby GD (1984) Enhancements of the SIMPLEC method for predicting incompressible fluid flows. *Numerical Heat Transfer* 7:147–163